

## Supporting Information

### **Branched cellulose reinforced composite polymer electrolyte with upgraded ionic conductivity for anode stabilized solid-state Li metal batteries**

Hailong Wu,<sup>a</sup> Jiali Wang,<sup>a</sup> Yu Zhao,<sup>a</sup> Xiaoqiang Zhang,<sup>a</sup> Ling Xu,<sup>a</sup> Hao Liu,<sup>c</sup> Yixiu Cui,<sup>a</sup>  
Yanhua Cui,<sup>a,\*</sup> and Chilin Li<sup>b,\*</sup>

<sup>a</sup> Institute of Electronic Engineering, China Academy of Engineering Physics, Mianyang 621000, China. Email: cuiyanhua@netease.com

<sup>b</sup> State Key Laboratory of High Performance Ceramics and Superfine Microstructure, Shanghai Institute of Ceramics, Chinese Academy of Sciences, Shanghai 200050, China. Email: chilinli@mail.sic.ac.cn

<sup>c</sup> Chengdu Green Energy and Green Manufacturing Technology R&D Center, Chengdu Science and Technology Development Center of CAEP, Chengdu, Sichuan 610207, China

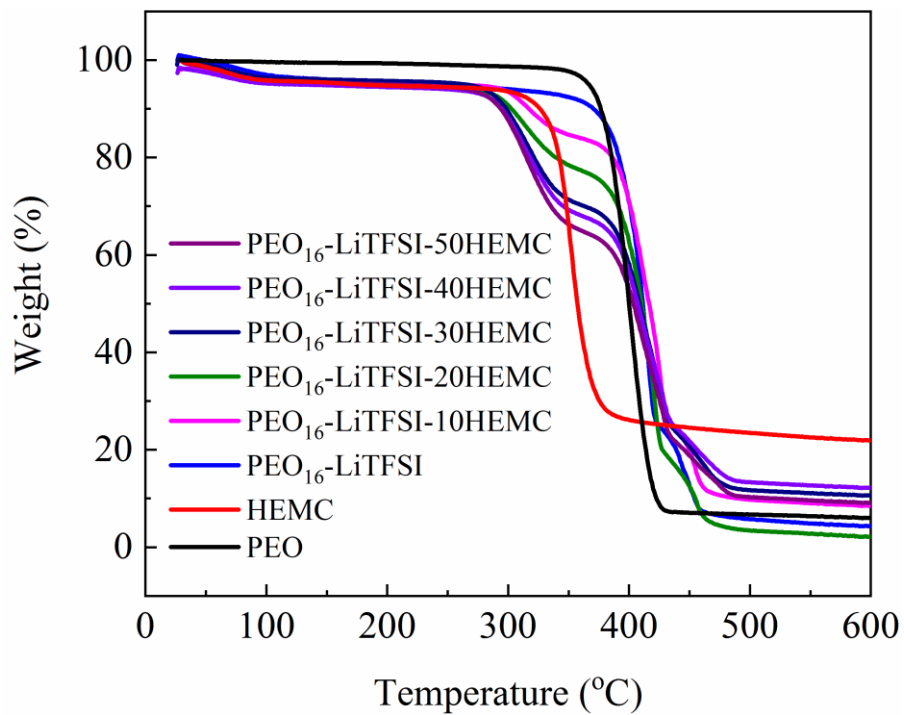


**Figure S1.** TGA curves of PEO, HEMC, PEO-SPE and PEO/HEMC-CPEs with HEMC filler of different content.

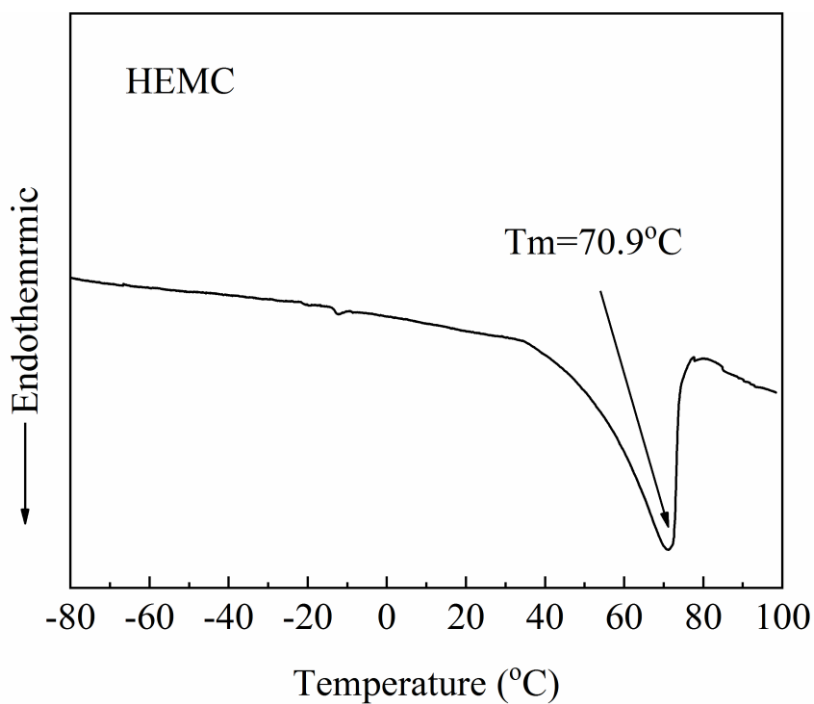


**Figure S2.** DSC thermogram of HEMC.

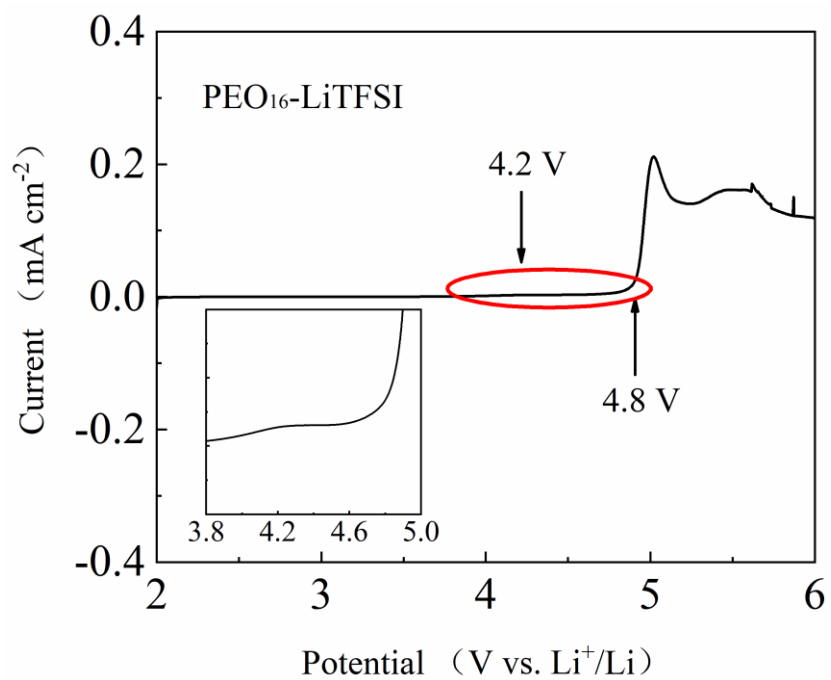


**Figure S3.** Liner sweep voltammogram of PEO-SPE with local magnification to disclose the position of current up-tilting as shown in inset.

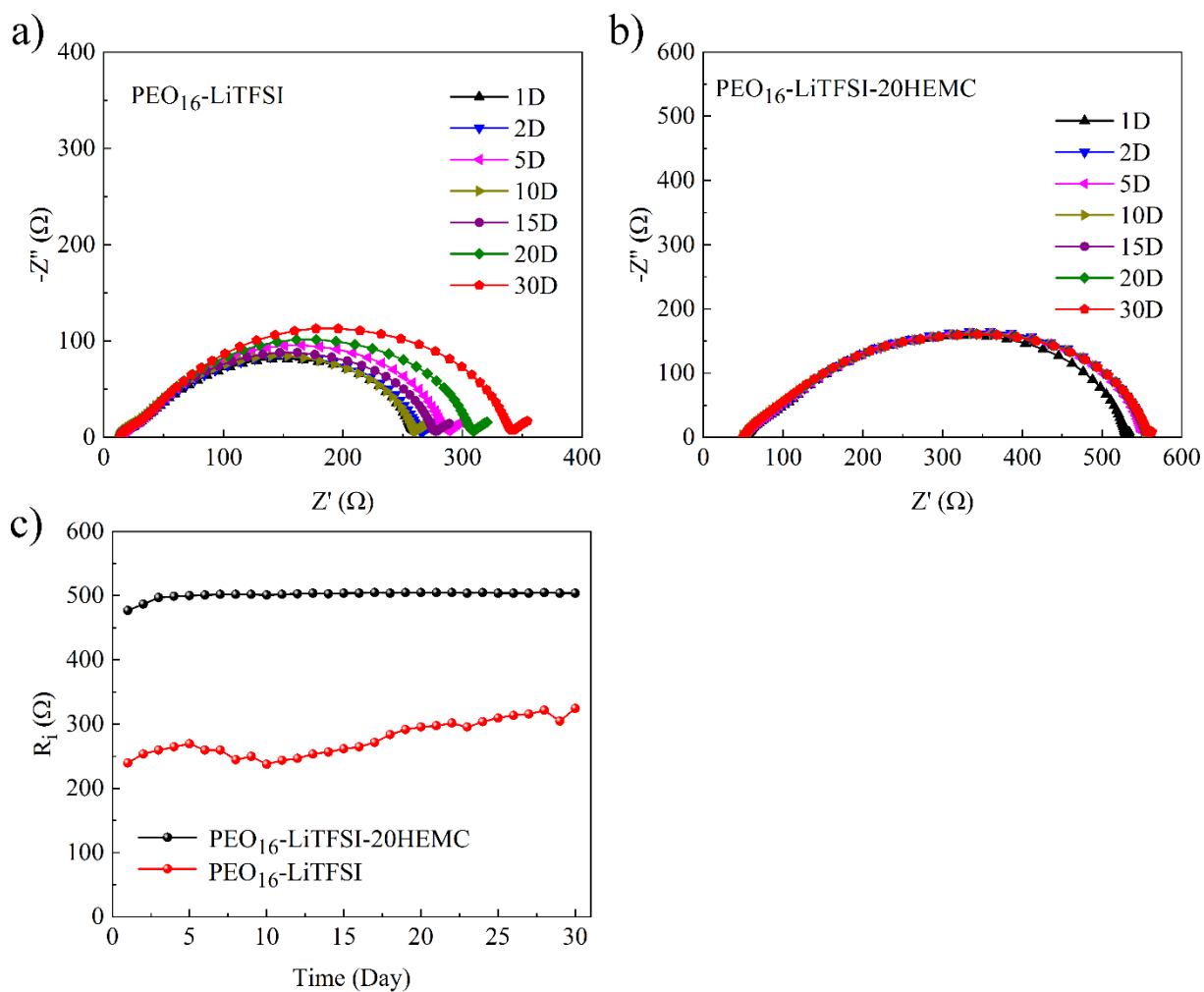


**Figure S4.** Impedance spectra of a)  $\text{Li}|\text{PEO}_{16}\text{-LiTFSI}|\text{Li}$  and b)  $\text{Li}|\text{PEO}_{16}\text{-LiTFSI-20HEMC}|\text{Li}$  symmetric cells for different aging time at 60 °C. c) Corresponding interfacial resistance evolution depending on different storage time.

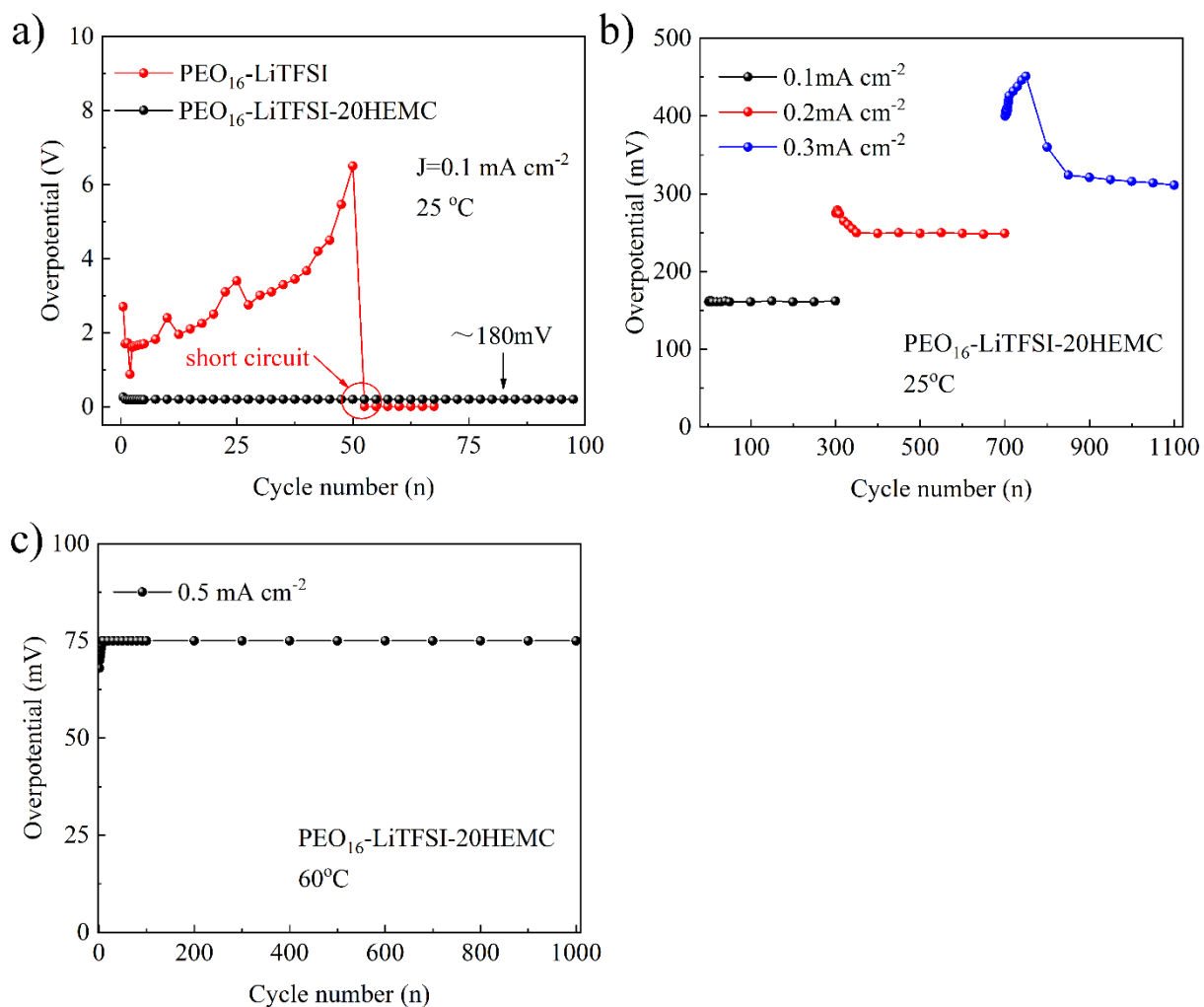


**Figure S5.** a) Overpotential comparison of  $\text{Li}|\text{PEO}_{16}\text{-LiTFSI}|\text{Li}$  and  $\text{Li}|\text{PEO}_{16}\text{-LiTFSI-20HEMC}|\text{Li}$  symmetric cells depending on cycle number at  $0.1 \text{ mA cm}^{-2}$  based on 1 h plating and 1 h stripping under room temperature. b) Overpotential evolution of  $\text{Li}|\text{PEO}_{16}\text{-LiTFSI-20HEMC}|\text{Li}$  symmetric cell under different current density of 0.1, 0.2 and  $0.3 \text{ mA cm}^{-2}$  as sequence under room temperature. c) Overpotential evolution of  $\text{Li}|\text{PEO}_{16}\text{-LiTFSI-20HEMC}|\text{Li}$  cell at a constant current density of  $0.5 \text{ mA cm}^{-2}$  under  $60 \text{ }^\circ\text{C}$ .

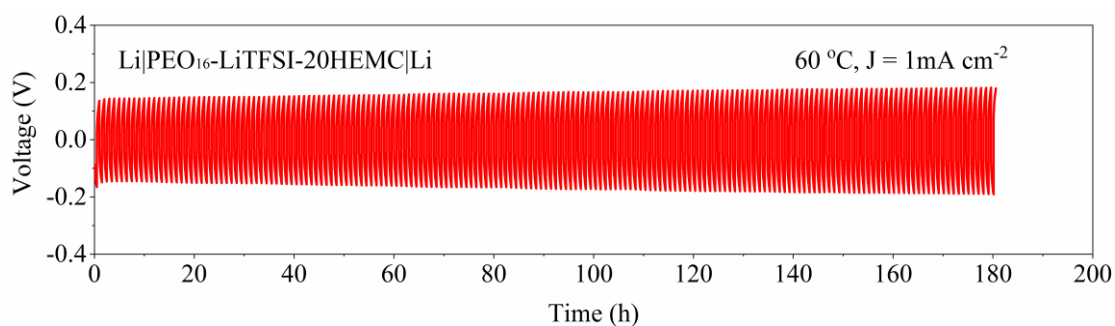


**Figure S6.** Galvanostatic cycling of Li|PEO<sub>16</sub>-LiTFSI-20HEMC|Li symmetrical cell based on a current density of 1 mA cm<sup>-2</sup> at 60 °C.

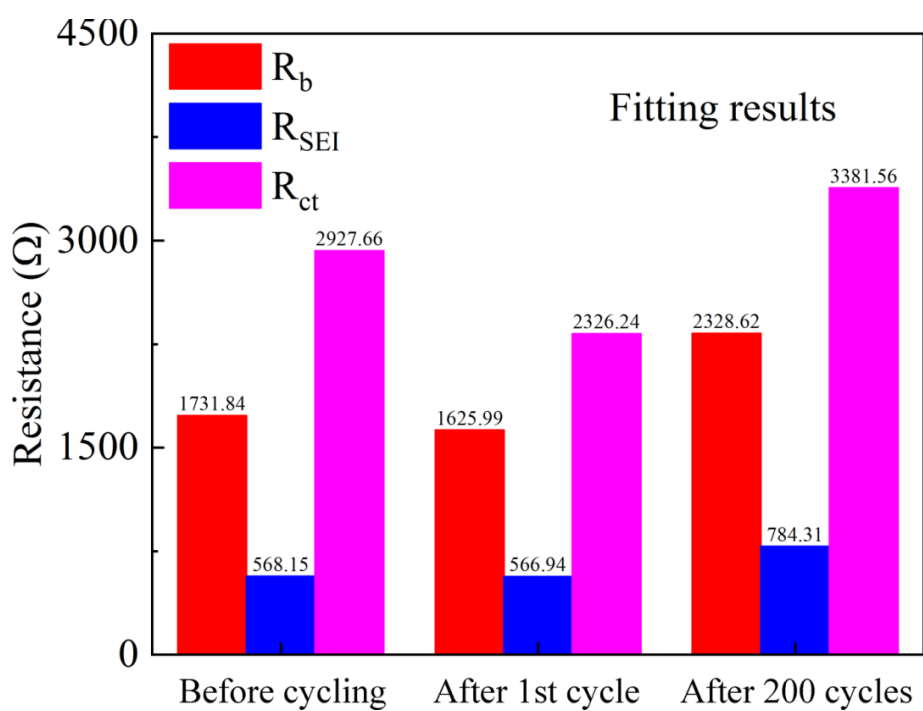


**Figure S7.** Fitting results of  $R_b$ ,  $R_{SEI}$  and  $R_{ct}$  values of Li|PEO<sub>16</sub>-LiTFSI-20HEMC|LiFePO<sub>4</sub> cell after different cycling stages at a current density of 0.5 C under ambient temperature.

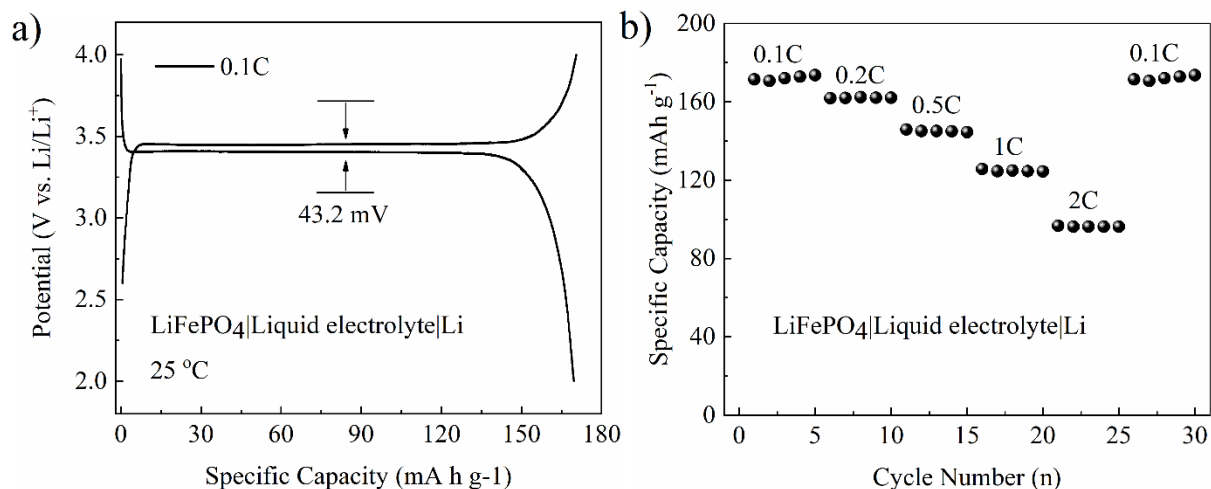


**Figure S8.** a) Typical charge-discharge curves and b) rate performance of Li|Liquid electrolyte|LiFePO<sub>4</sub> cell operated at ambient temperature.

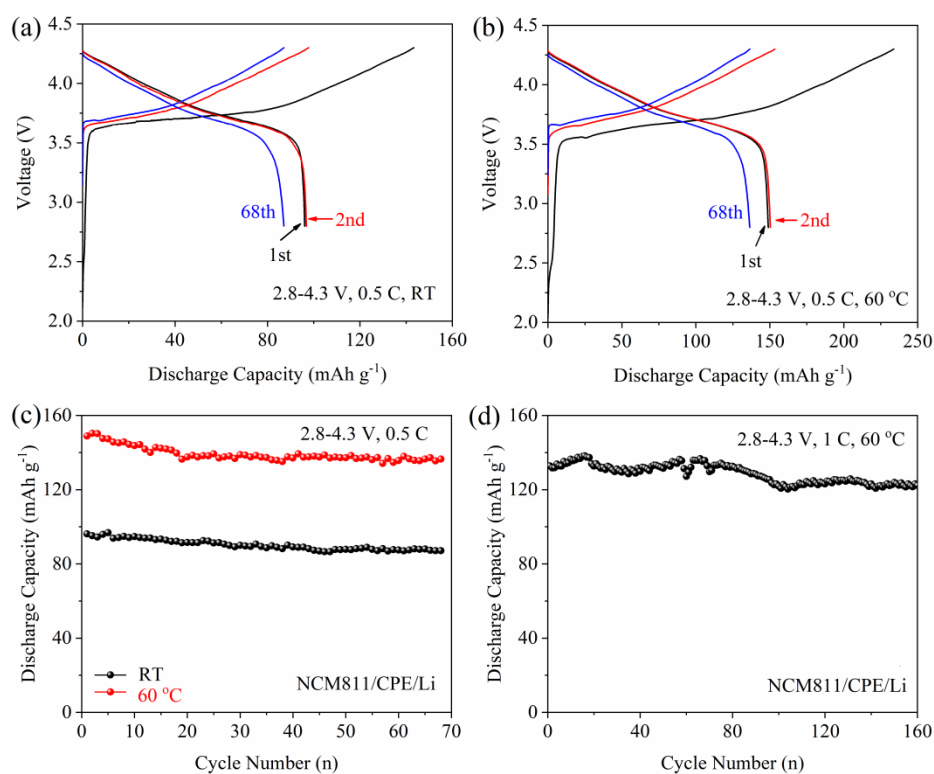


**Figure S9.** Charge-discharge profiles of Li/PEO<sub>16</sub>-LiTFSI-20HEMC/NCM811 cells in different cycling stages at 0.5 C measured at (a) room temperature and (b) 60 °C. Cycling performance of Li/PEO<sub>16</sub>-LiTFSI-20HEMC/NCM811 cells (c) at 0.5 C measured at room temperature and 60 °C and (d) at 1 C measured at 60 °C.